Synthesis of transparent dispersions of aluminium hydroxide nanoparticles

IOP Publishing Nanotechnology
Nanotechnology 29 (2018) 305605 (7pp) https://doi.org/10.1088/1361-6528/aac371

Synthesis of transparent dispersions of aluminium hydroxide nanoparticles

Bo Chen[1,2,3], Jie-Xin Wang[1,2,4,5], Dan Wang[1,2,4], Xiao-Fei Zeng[1,2], Stuart M Clarke[3,5] and Jian-Feng Chen[1,2,4]

[1] State Key Laboratory of Organic-Inorganic Composites, Beijing University of Chemical Technology, Beijing, 100029, People's Republic of China
[2] Research Center of the Ministry of Education for High Gravity Engineering and Technology, Beijing University of Chemical Technology, Beijing, 100029, People's Republic of China
[3] BP Institute and Department of Chemistry, University of Cambridge, Cambridge, CB2 1EW, United Kingdom
[4] Beijing Advanced Innovation Center for Soft Matter Science and Engineering, Beijing University of Chemical Technology, Beijing, 100029, People's Republic of China

E-mail: wangjx@mail.buct.edu.cn and stuart@bpi.cam.ac.uk

Received 19 March 2018, revised 4 May 2018
Accepted for publication 9 May 2018
Published 23 May 2018

Abstract

Transparent dispersions of inorganic nanoparticles are attractive materials in many fields. However, a facile method for preparing such dispersions of aluminium hydroxide nanoparticles is yet to be realized. Here, we report a direct reactive method to prepare transparent dispersions of pseudo-boehmite nanoparticles (1 wt%) without any surface modification, and with an average particle size of 80 nm in length and 10 nm in width, as well as excellent optical transparency over 94% in the visible range. Furthermore, transparent dispersions of boehmite nanoparticles (1.5 wt%) were also achieved after an additional hydrothermal treatment. However, the optical transparency of dispersions decreased with the rise of hydrothermal temperature and the shape of particles changed from rhombs to hexagons. In particular, monodisperse hexagonal boehmite nanoplates with an average lateral size of 58 nm and a thickness of 12.5 nm were obtained at a hydrothermal temperature of 220 °C. The selectivity of crystal growth direction was speculated as the possible formation mechanism of these as-prepared aluminium hydroxide nanoparticles. Besides, two values of 19.6 wt% and 14.64 wt% were separately measured for the weight loss of pseudo-boehmite and boehmite nanoparticles after a continuous heating, indicating their potential flame-resistant applications in the fabrication of plastic electronics and optical devices with high transparency.

Keywords: transparent dispersions, pseudo-boehmite, boehmite, monodisperse nanoparticles, flame-resistant

(Some figures may appear in colour only in the online journal)

1. Introduction

In the past few decades, nanostructures and nanomaterials, which exhibit many unique physical and chemical properties, have been widely investigated for both their scientific and industrial applications [1–3]. Nanopowders are being used in a number of fields, such as photocatalyst, magnetics, biology and medicine [4–6]. Among these applications is the use of nanocomposites, where the nanopowders are dispersed in a continuous matrix [7, 8]. However, nanopowders without surface modification usually aggregate easily, which may lead to deterioration of the mechanical properties of nanocomposites, and shorten their working life [9]. Hence, it is important to enhance the particle dispersibility, to prepare high-performance nanomaterials, such as optical devices, self-assembled materials, pharmaceuticals and catalysts [10–12].

[5] Authors to whom any correspondence should be addressed.

Nanoparticles in dispersions have a better dispersibility than nanopowders, so they are ideal replacements of nanopowders in many industrial applications [13]. There are numerous kinds of dispersions of nanoparticles that have been successfully prepared, including noble metals (Pt, Pd, Au, Ag, etc) [14, 15], metal oxides (ZnO, ZrO_2, CuO, TiO_2, etc) [16, 17], magnetic and dielectric materials (Fe_3O_4, $MnFe_2O_4$, $CoFe_2O_4$, $BaTiO_3$, etc) [18, 19], and metal hydroxides ($Ca(OH)_2$, MgAl-LDH, etc) [20, 21]. Among them, transparent dispersion of monodisperse metal hydroxide nanoparticles has been seldom reported so far.

Pseudo-boehmite ($AlOOH \cdot nH_2O$, $n = 0.08$–0.62) and boehmite (γ-AlOOH) are two important kinds of aluminium hydroxides (ATH). ATH nanoparticles can be applied in a lot of fields. For example, they have been used as high-efficiency and green flame retardants in polymers owing to their nontoxicity, high decomposition temperature and smoke suppression [22]. They are also the best precursors for the synthesis of high-quality nanosized γ-Al_2O_3 [23]. In addition, they can be also adopted as adsorbents to treat acidoids, thus providing cost-effective solutions to environmental problems [24]. Presently, the commonly used preparation methods for ATH nanoparticles are hard to achieve ATH nanoparticles with good dispersity or even monodispersity [25, 26]. Therefore, it is of great significance to develop a facile method to prepare transparent dispersions of monodisperse ATH nanoparticles.

In our previous study, transparent dispersions of magnesium hydroxide (MH) nanoparticles using a surface modification method were reported [27]. However, this method required the introduction of a silane coupling agent, and the resulting hydrophobic surface of MH nanoparticles significantly limited the application field of products. In this article, a more straightforward procedure was carried out to prepare transparent dispersions of ATH nanoparticles, including pseudo-boehmite nanoparticles obtained by a direct precipitation method and monodisperse hexagonal boehmite nanoplates achieved after an additional hydrothermal treatment. To the best of our knowledge, it is the first time that transparent and stable dispersions of ATH nanoparticles have been prepared without any surface modification. The possible formation mechanism was also investigated.

2. Experimental section

2.1. Materials

Aluminium chloride hexahydrate ($AlCl_3 \cdot 6H_2O$, $\geqslant 98\%$), sodium hydroxide (NaOH, $\geqslant 98\%$), ethanol (C_2H_5OH, $\geqslant 99.8\%$) and ethylene glycol ($C_2H_4(OH)_2$, $\geqslant 99.8\%$) were purchased from Beijing Chemical Reagent Co., Ltd. (China). All the chemical reagents used in these experiments were analytically pure and without any further purification. Deionized water (18.2 MΩ cm) was produced by a Hitech-K Flow Water Purification System from Hitech Instruments Co., Ltd (China).

2.2. Preparation of transparent dispersions of ATH nanoparticles

Transparent dispersions of pseudo-boehmite nanoparticles were prepared by a direct precipitation method. Typically, 2.41 g of $AlCl_3 \cdot 6H_2O$ and 1.19 g of NaOH were each dissolved in separate 100 ml of deionized water to form solution A and solution B, respectively. Solution A was kept in a flask at room temperature and solution B was added dropwise into solution A to generate a mixed slurry under a violent stirring. Afterwards, the mixed slurry was heated to 70 °C and maintained for 2 h. The resulting slurry was filtered, washed with deionized water and the dispersion medium (deionized water, ethanol or ethylene glycol) several times, and finally suspended in the dispersion medium.

Transparent dispersions of boehmite nanoparticles were prepared by a following hydrothermal treatment. Typically, the above slurry was filtered, washed with deionized water several times, and then redispersed into 60 ml of deionized water. Afterwards, the dispersion was transferred into a 100 ml teflon-lined stainless steel autoclave and the autoclave was sealed and placed in an oven at a particular temperature for 12 h. Finally, the oven was cooled down to room temperature and the resulting dispersion was recovered.

2.3. Characterization

The x-ray diffraction (XRD) patterns of ATH nanoparticles were recorded using an x-ray diffractometer (XRD-6000, Shimadzu, Japan). The Fourier transform infrared (FT-IR) spectra of ATH nanoparticles were measured by a Nicolet 6700 spectrometer (Nicolet Instrument Co., USA) in the range of 4000–400 cm^{-1}. The sizes and morphologies of ATH nanoparticles were observed on a transmission electron microscope (TEM) (JEM-2010F, JEOL, Japan) and an atomic force microscope (AFM) (Dimension 3100, Veeco Instrument Co., USA). The optical transparency of ATH dispersions was assessed using a UV–vis spectrometer (UV-2501, Shimadzu, Japan) in the range of 200–800 nm. The zeta potential of pseudo-boehmite nanoparticles dispersed in aqueous solution was detected through a zeta potential analyzer (Nano ZS-90, Malvern Instrument Ltd., UK). The rheology test for pseudo-boehmite aqueous dispersion was performed by a Kinexus DSR (Malvern Instrument Ltd., UK) at 25 °C. The thermal behavior of ATH nanoparticles was investigated via a thermal gravimetric analysis (TGA) system (TGA/DSC1 SF 1100, Mettler Toledo, Switzerland) at a heating rate of 10 °C min^{-1} in air.

3. Results and discussion

Figure 1 shows the representative XRD patterns of ATH nanoparticles prepared without a hydrothermal step and those with a hydrothermal step at different temperatures. Clearly, the product prepared without a hydrothermal step (curve (a)) showed all characteristic peaks of pseudo-boehmite (JCPDS 21-1307) [28]. Furthermore, no impurity peaks were detected,

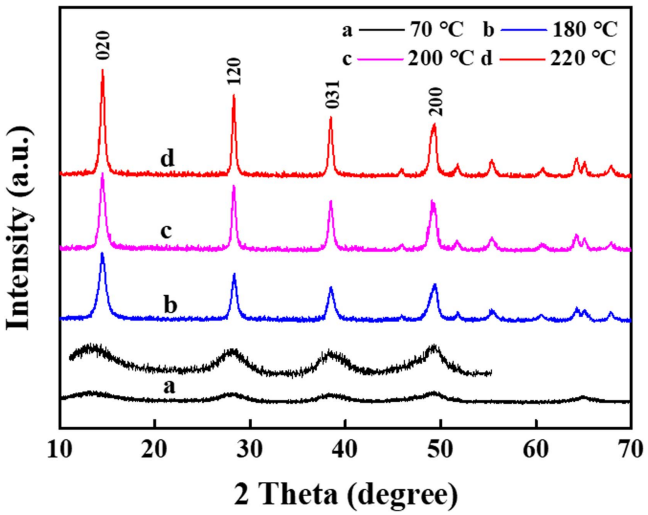

Figure 1. XRD patterns of ATH nanoparticles prepared (a) without a hydrothermal step at 70 °C; (b) with a hydrothermal step at 180 °C; (c) with a hydrothermal step at 200 °C; (d) with a hydrothermal step at 220 °C.

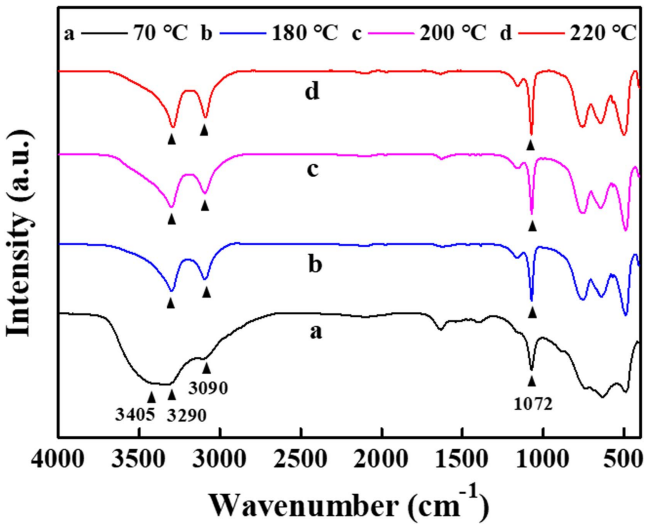

Figure 2. FT-IR spectra of ATH nanoparticles prepared (a) without a hydrothermal step at 70 °C; (b) with a hydrothermal step at 180 °C; (c) with a hydrothermal step at 200 °C; (d) with a hydrothermal step at 220 °C.

indicating that pure pseudo-boehmite nanoparticles were obtained. However, the diffraction peaks at (020), (120), (031) and (200) lattice planes were dramatically strengthened and sharpened for the hydrothermally prepared ATH nanoparticles (curve (b)–(d)), and notably, the diffraction peak at (020) shifted to a higher degree, which was ascribed to a smaller $d_{(020)}$, according to Bragg's law. These results indicated that pseudo-boehmite nanoparticles were transformed into boehmite nanoparticles after the hydrothermal treatment, corresponding to the previous studies by Santos *et al* [29]. In addition, the intensity of peaks increased gradually and the width of peaks decreased slightly with an increase on the hydrothermal temperature, suggesting that higher temperature resulted in higher crystallinity and larger particle size.

Figure 2 presents the corresponding FT-IR spectra of four samples. It could be found that they all exhibited a sharp and strong peak at 1072 cm^{-1}, owing to the bending vibration of Al–OH. Besides, two peaks were measured at 3290 cm^{-1} and 3090 cm^{-1}, respectively, corresponding to the symmetric and asymmetric stretching vibrations of O−H. All peaks appeared at 750–480 cm^{-1} should be assigned to the stretching and bending vibrations of Al−O. Clearly, these curves indicated that the as-prepared samples consisted of AlOOH. However, a broad peak from the sample without a hydrothermal step at 3405 cm^{-1} disappeared after the hydrothermal treatment. This peak was mainly attributed to the stretching vibration of O−H in water, demonstrating the existence of crystal water in sample (a), but not in sample (b)–(d). This result confirmed that pseudo-boehmite and boehmite nanoparticles were achieved before and after the hydrothermal treatment, further supporting the XRD results.

Figure 3 displays the typical TEM and AFM images of ATH nanoparticles, and the corresponding visual photograph of ATH nanoparticles dispersed in water with a solid content of 1.5 wt%. From figure 3(a), pseudo-boehmite nanoparticles were obtained with irregular shapes, having an average particle size of about 80 nm in length and 10 nm in width. Compared with the irregular-shaped pseudo-boehmite nanoparticles, lath-like boehmite nanoparticles with jagged borders (figure 3(b)), plate-like boehmite nanoparticles with rhomb shapes (figure 3(c)), and hexagonal boehmite nanoplates (figure 3(d)) were respectively obtained at different hydrothermal temperatures. Obviously, the particle size increased with the hydrothermal temperature and the morphology became more and more regular. As shown in figure 3(c), most particles were still connected to each other and formed head-to-tail chains, when the hydrothermal temperature was raised to 200 °C. However, after a further rise of temperature to 220 °C, these particles would separate from each other and turned into monodisperse hexagonal nanoplates. These hexagonal nanoplates were obtained with a very narrow size distribution, and had an average lateral size of 58 nm and a thickness of 12.5 nm (figure 3(e)). Apparently, the optical transparency of ATH dispersions decreased gradually with the rise of hydrothermal temperature (figure 3(f)), mainly due to the increase of particle size.

Figure 4 gives a schematic diagram of the possible formation mechanism of the obtained ATH nanoparticles. In general, high temperature usually facilitates the recrystallization of particles from poorly-crystallized to well-crystallized, or even from amorphous structures to crystals. As a result, the hydrothermal process at high temperature over 180 °C in this study triggered the transformation of amorphous pseudo-boehmite nanoparticles to well-crystallized boehmite nanoparticles (figure 4(a)), which was also proved by XRD and FT-IR results. Besides, well-crystallized boehmite is composed of octahedral layers with orthorhombic structure, and the crystalline structure is defined by the (010) plane, the basal plane of AlOOH crystals [30]. Therefore, the obtained boehmite nanoparticles showed a tendency to grow along the direction parallel to the (010) plane and formed hexagonal shapes, which was an ideal pathway for these particles to form layered

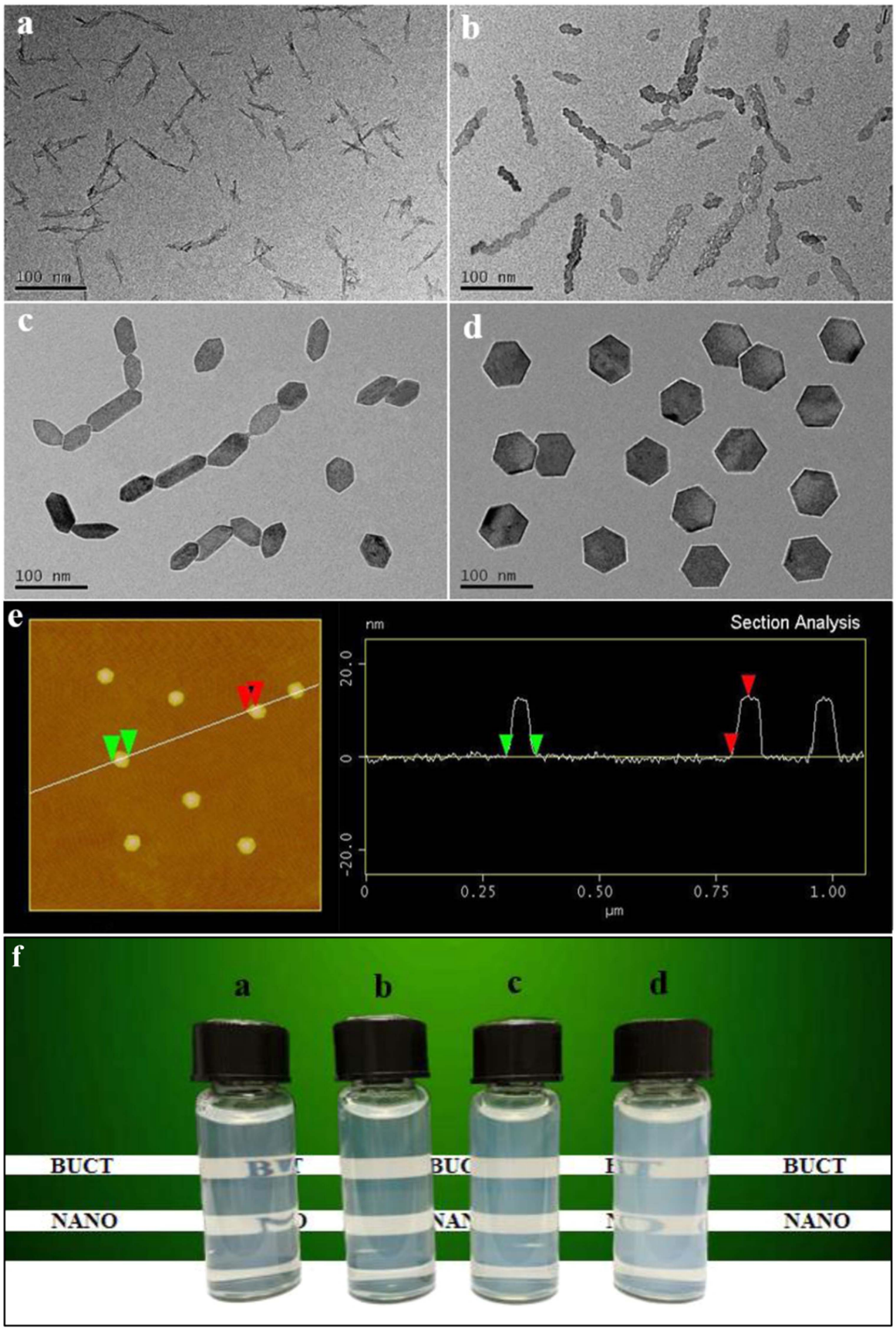

Figure 3. TEM images of ATH nanoparticles prepared (a) without a hydrothermal step at 70 °C; (b) with a hydrothermal step at 180 °C; (c) with a hydrothermal step at 200 °C; (d) with a hydrothermal step at 220 °C; and (e) AFM image of boehmite nanoparticles prepared at 220 °C; (f) the corresponding visual photograph of the as-prepared ATH nanoparticles dispersed in water with a solid content of 1.5 wt%.

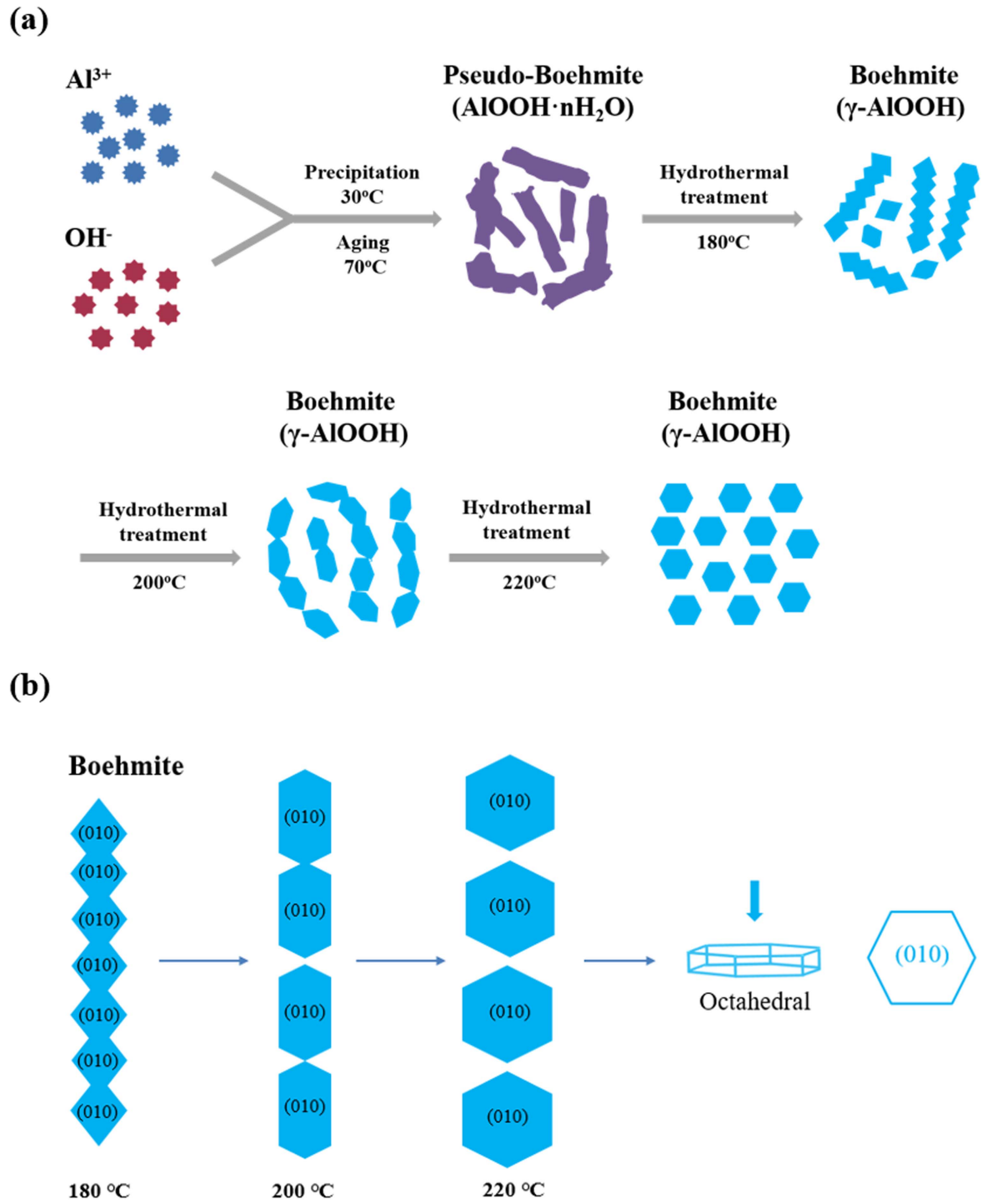

Figure 4. The possible formation mechanism of the obtained ATH nanoparticles.

octahedral structure. Correspondingly, the morphology of boehmite nanoparticles changed from the initial rhombs to the final hexagons was due to the selectivity of crystal growth direction (figure 4(b)).

Figure 5 shows UV–vis spectra and the corresponding visual photograph (inset) of pseudo-boehmite nanoparticles dispersed in ethylene glycol (EG), ethanol (EA), and deionized water (WT) with a solid content of 1 wt%. From the UV–vis result, it could be clearly seen that all of three samples showed excellent optical transparency with the visible light transmittance over 94% at 760 nm. Compared with the aqueous dispersion and ethanol dispersion, the ethylene glycol dispersion was achieved with a better transparency in the visible range of 380–760 nm. This result could be explained by considering the factors that control light scattering of small particles and the refractive index matching between nanoparticles and the surrounding dispersion medium. According to Rayleigh scattering, the intensity of scattered light declines rapidly with the decrease of particle size, and resulting in the increasing visible light transmittance. Previous fundamental

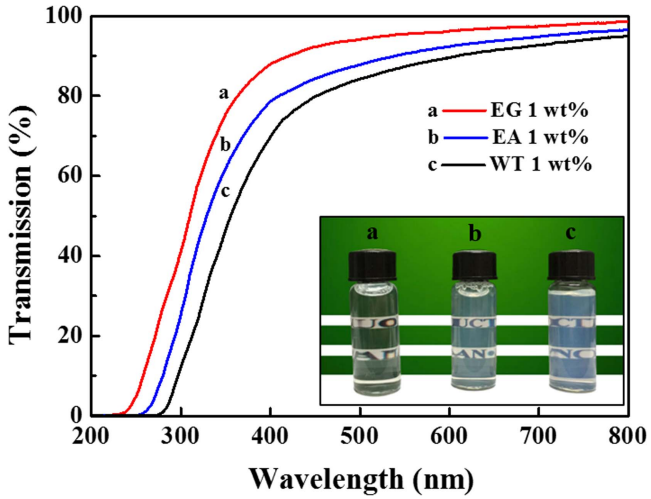

Figure 5. UV–vis spectra and the corresponding visual photograph (inset) of pseudo-boehmite nanoparticles dispersed in (a) ethylene glycol (EG); (b) ethanol (EA); (c) deionized water (WT) with a solid content of 1 wt%.

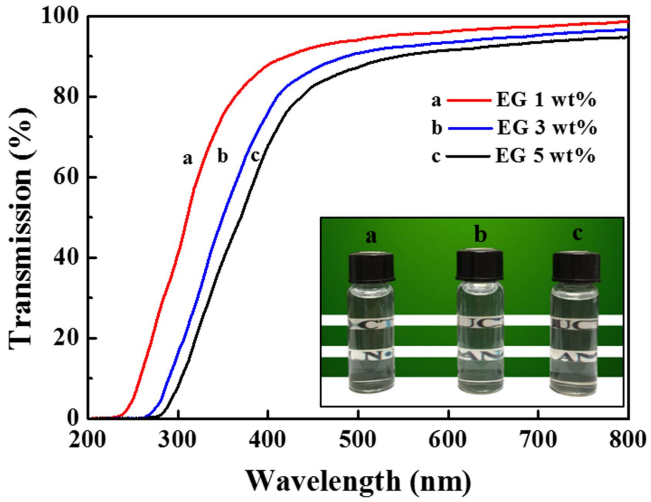

Figure 6. UV–vis spectra and the corresponding visual photograph (inset) of pseudo-boehmite nanoparticles dispersed in ethylene glycol with a solid content of (a) 1 wt%; (b) 3 wt%; (c) 5 wt%.

study also proved that particle size smaller than 40 nm is beneficial to obtain transparent nanomaterials [31], confirming the obtained small particle size contributed to the high transparency of dispersions. In addition, ethylene glycol has a closer refractive index ($n_D = 1.43$) to pseudo-boehmite nanoparticles ($n_D = 1.64$), compared with ethanol ($n_D = 1.36$) and water ($n_D = 1.33$), thus giving rise to a better performance in optical transparency.

Zeta potential analysis was applied to investigate the surface charge of pseudo-boehmite nanoparticles dispersed in dispersions. A value of +54.2 mV was obtained for the pseudo-boehmite aqueous dispersion. Generally, dispersions with good stability can be prepared by increasing the zeta potential to 40 mV or higher [32]. Therefore, it was supposed that the obtained high zeta potential made a contribution to

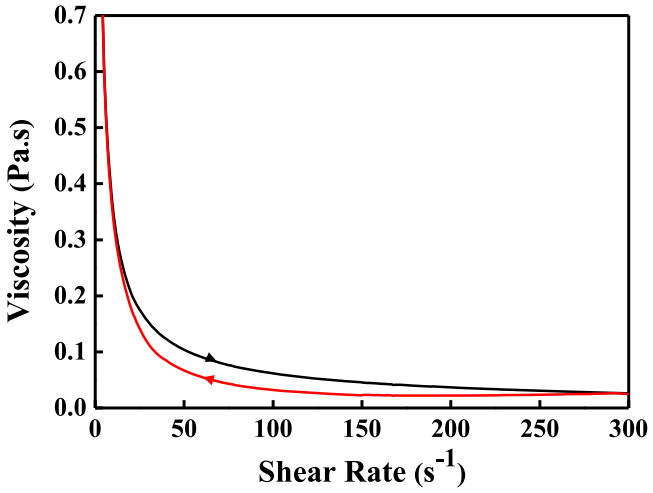

Figure 7. The rheology test for the dispersion of pseudo-boehmite nanoparticles with a solid content of 3 wt% at 25 °C.

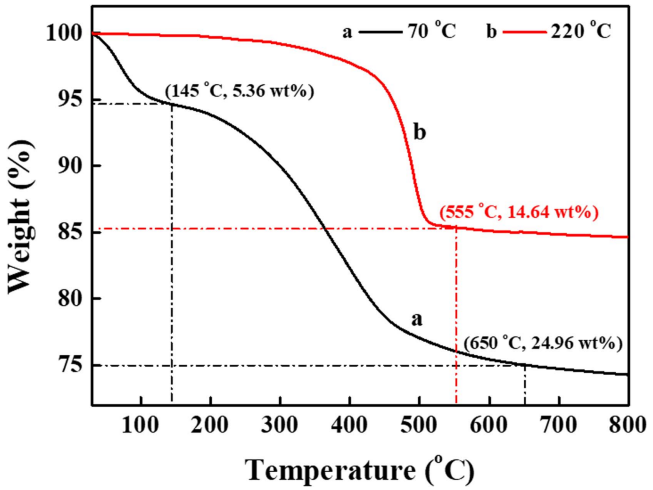

Figure 8. TG curves of ATH nanoparticles prepared (a) without a hydrothermal step at 70 °C; (b) with a hydrothermal step at 220 °C.

the formation of stable dispersions, in spite of no surface modification.

Figure 6 displays UV–vis spectra and the corresponding visual photograph (inset) of pseudo-boehmite nanoparticles dispersed in ethylene glycol (EG) with different solid contents. Obviously, all of these different solid content samples exhibited excellent optical transparency. The visible light transmittance at 760 nm reached up to 94.2% even if the solid content was raised to 5 wt%. Nevertheless, the fluidity of these dispersions deteriorated quickly with the increase of solid content, because of the thixotropy of pseudo-boehmite dispersions, as proved by the rheology test (figure 7). The limit of solid content in these experiments was found to be 7.2 wt%.

Figure 8 shows TG curves of ATH nanoparticles prepared without a hydrothermal step and those with a hydrothermal step at 220 °C. As shown in curve (a), a two-step weight loss happened to the pseudo-boehmite nanoparticles. The first weight loss step was in the range of 30 °C–145 °C,

corresponding to a value of 5.36 wt%. This was mainly attributed to the removal of surface absorbed water. The second weight loss step with a value of 19.6 wt% was detected from 145 °C to 650 °C, accounting for the decomposition of $AlOOH \cdot nH_2O$ ($n = 0.08$–0.62). This value could be used to calculate the number of '*n*', which was finally determined as 0.24 if the decomposition was complete. In contrast, the boehmite nanoparticles exhibited a continuous weight loss from 300 °C to 550 °C (curve (b)), giving a final weight loss of 14.64 wt%. This value was slightly lower than the theoretical value of totally complete decomposition of AlOOH (15 wt%), indicating that these particles were obtained with a complete crystallization and less deficiency in crystal lattice. According to TG results, the as-prepared transparent dispersions of ATH nanoparticles have a good prospect as green and highly-efficient flame retardants in optical devices, electronic devices, etc.

4. Conclusions

In summary, transparent dispersions of pseudo-boehmite nanoparticles with an average particle size of about 80 nm in length and 10 nm in width were successfully prepared without any surface modification by a direct precipitation method. Besides, transparent dispersions of boehmite nanoparticles were also achieved by a following hydrothermal treatment. The lateral size of boehmite nanoparticles increased with the rise of hydrothermal temperature, and the particle shape became more and more regular. In particular, monodisperse hexagonal boehmite nanoplates with an average lateral size of 58 nm and a thickness of 12.5 nm were obtained at a hydrothermal temperature of 220 °C. Based on the as-prepared ATH nanoparticles, the possible formation mechanism was also explored in the view of selectivity of crystal growth direction. UV–vis results indicated that the optical transparency of pseudo-boehmite dispersions could be as high as 94% in the visible range, however, a gradual decline happened to the boehmite dispersions after the hydrothermal treatment. Both the pseudo-boehmite nanoparticles and boehmite nanoparticles showed an evident weight loss after a continuous heating, suggesting that the as-prepared transparent dispersions of ATH nanoparticles have a great potential as green and highly-efficient flame retardants in optical devices, electronic devices, etc.

Acknowledgments

This work was financially supported by the National Natural Science Foundation of China (21576022 and 21622601) and the National Key Research and Development Program of China (2016YFA0201701/2016YFA0201700).

ORCID iDs

Jie-Xin Wang https://orcid.org/0000-0002-1854-4095
Dan Wang https://orcid.org/0000-0002-3515-4590

References

[1] Stupp S I 2016 *Chem. Rev.* **105** 1023–4
[2] Tan C L *et al* 2017 *Chem. Rev.* **117** 6225–31
[3] Choi S, Lee H, Ghaffari R, Hyeon T and Kim D H 2016 *Adv. Mater.* **28** 4203–18
[4] Tong H, Ouyang S, Bi Y, Umezawa N, Oshikiri M and Ye J H 2012 *Adv. Mater.* **24** 229–51
[5] Rücker U 2011 *Adv. Phys.* **47** 511–97
[6] Wen A M and Steinmetz N F 2016 *Chem. Soc. Rev.* **45** 4074–126
[7] Cannas C, Musinu A D, Peddis A D and Piccaluga G 2006 *Chem. Mater.* **18** 3835–42
[8] Gharagozlou M, Ramezanzadeh B and Baradaran Z 2016 *Appl. Surf. Sci.* **377** 86–98
[9] Li D and Kaner R B 2006 *J. Am. Chem. Soc.* **128** 968–75
[10] Cohen E, Weissman H, Pinkas I, Shimoni E, Rehak P, Král P and Rybtchinski B 2017 *ACS Nano* **12** 317–26
[11] Zhang D, Quayle M J, Petersson G, Ommen J R V and Folestad 2017 *Nanoscale* **9** 11410–7
[12] Yoo E J, Okata T, Akita T, Kohyama M, Nakamura J and Honma I 2009 *Nano Lett.* **9** 2255–9
[13] Cheng F Y, Su C H, Yang Y S, Yeh C S, Tsai C Y, Wu C L, Wu M T and Shieh D B 2005 *Biomaterials* **26** 729–38
[14] Wang X and Li Y D 2007 *Chem. Commun.* **28** 2901–10
[15] Han X W, Zeng X F, Zhang J, Huan H F, Wang J X, Foster N R and Chen J F 2016 *Chem. Eng. J.* **296** 182–90
[16] Dou Q and Ng K M 2016 *Powder Technol.* **301** 949–58
[17] Balasubramanian B, Kraemer K L, Reding N A, Skomski R, Ducharme S and Sellmyer D J 2010 *ACS Nano* **4** 1893–900
[18] Sun S H, Zeng H, Robinson D B, Raoux S, Rice P M, Wang S X and Li G X 2004 *J. Am. Chem. Soc.* **126** 273–9
[19] Liang X, Wang X, Zhuang J, Cheng Y T, Wang D S and Li Y D 2010 *Adv. Funct. Mater.* **16** 1805–13
[20] Rodrigueznavarro C, Suzuki A and Ruizagudo E 2013 *Langmuir* **29** 11457–70
[21] Xu Z P, Stevenson G, Lu C Q and Lu G Q 2006 *J. Phys. Chem.* B **110** 16923–9
[22] Cai Y H, Zhao M M, Wang H T, Li Y J and Zhao Z G 2014 *Polym. Degrad. Stabil.* **99** 53–60
[23] Wang S, Li X, Wang S and Zhai Y 2008 *Mater. Lett.* **62** 3552–4
[24] Yujiro W, Takeshi K, Keisuke F, Toshiyuki I, Yu K and Junzo T 2011 *Sep. Sci. Technol.* **46** 818–24
[25] Ohta Y, Hayakawa T, Inomata T, Ozawa T and Masuda H 2017 *J. Nanopart. Res.* **19** 232–45
[26] Jiang Z Q, Ma H W, Yang J and Wang L 2013 *Adv. Mater. Res.* **684** 46–52
[27] Wang J X, Sun Q, Chen B, Wu X, Zeng X F, Zhang C, Zou H K and Chen J F 2015 *Nanotechnology* **26** 195602–9
[28] Wang Y J, Xu D Q, Sun H T and Luo G S 2011 *Ind. Eng. Chem. Res.* **50** 3889–94
[29] Santos P D S, Coelho A C V, Santos H D S and Kiyohara P K 2009 *Mater. Res.* **12** 437–45
[30] Jiao W Q, Wu X Z, Xue T, Li G, Wang W W, Wang Y X, Wang Y M, Tang Y and He M Y 2016 *Cryst. Growth Des.* **16** 5166–73
[31] Althues H, Henle J and Kaskel S 2007 *Chem. Soc. Rev.* **36** 1454–65
[32] Barner A and Myers M 2013 *J. Eur. Ceram. Soc.* **32** 235–44